ChemComm

COMMUNICATION

View Article Online
View Journal | View Issue

Cite this: *Chem. Commun.*, 2015, **51**, 13779

Received 16th June 2015,
Accepted 16th July 2015

DOI: 10.1039/c5cc04971g

www.rsc.org/chemcomm

Evidence of rutile-to-anatase photo-induced electron transfer in mixed-phase TiO_2 by solid-state NMR spectroscopy†

Xiaoming Sun,[ac] Weili Dai,[a] Guangjun Wu,[a] Landong Li,*[ab] Naijia Guan[ab] and Michael Hunger*[c]

With ethanol as a probe molecule, the surface sites of anatase and rutile can be distinguished using ^{13}C CP/MAS NMR spectroscopy, which offers an opportunity to investigate the transfer of photo-induced electrons from rutile to anatase in the mixed-phase TiO_2.

Semiconductor photocatalysis has attracted significant attention for decades since the discovery of water photolysis on a TiO_2 photoanode by Fujishima and Honda.[1] Although TiO_2 is the initial and the most investigated semiconductor photocatalyst, some key issues on TiO_2 photocatalysis are still to be resolved, which could significantly improve the current understanding of the photocatalytic material and process. It is well known that the crystalline structure shows great impacts on the photocatalytic performance of TiO_2. The two major crystalline phases of TiO_2 investigated as photocatalysts are anatase and rutile, with a band gap of *ca.* 3.2 and 3.0 eV, respectively.[2] Since rutile is the most chemically stable phase of TiO_2, anatase is generally regarded as the more active phase than rutile.[3] Meanwhile, the mixed-phase TiO_2 such as commercial Degussa P25 was found to exhibit enhanced photocatalytic properties in contrast to the individual phase TiO_2.[4] For example, Li and co-workers introduced the concept of the anatase/rutile phase junction, and proposed that the formation of a surface junction is responsible for the enhanced photocatalytic activity of mixed-phase TiO_2.[4a] Charge separation could be achieved in the anatase/rutile phase junction and the prolonged lifetime of charge carriers would lead to an improved photocatalytic activity. In this context, the determination of the charge transfer process at the anatase/rutile phase junction is of great significance to reveal the role of each phase in the junction and also to design robust photocatalysts with high efficiencies. In fact, other robust heterojunction systems, *e.g.* α-Ga_2O_3/β-Ga_2O_3 and CN/CSN, have been successfully fabricated for semiconductor photocatalysis.[5]

To explain the synergetic effect between anatase and rutile in the phase junction, numerous efforts have been devoted.[6–10] However, the discussed models of the direction of interfacial charge transfer and the energetic alignment of the band edges of anatase and rutile are somewhat controversial. Conventionally, the conduction band of anatase was established to be ~0.2 eV higher than that of rutile according to the flatband potential measurements, which corresponds to the aligned valence band maxima (Fig. 1a).[6] As a result, the photo-induced electrons would preferentially transfer from anatase to rutile, while the holes from rutile to anatase. This alignment is generally acknowledged in early studies and also supported by some pieces of theoretical and experimental evidence.[7] In contrast, the results of the electron paramagnetic resonance spectroscopy indicated the transfer of photo-induced electrons from rutile to anatase.[8] A series of theoretical studies also proposed a staggered band

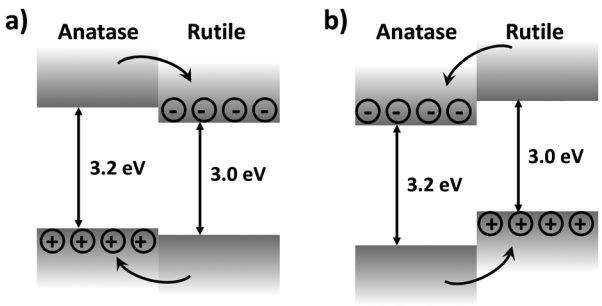

Fig. 1 The two models proposed for the energetic alignment of the band edges of anatase and rutile in the mixed-phase TiO_2: (a) conventional configuration with the conduction band of anatase above rutile and the anatase-to-rutile photo-induced electron transfer; (b) recent configuration with the conduction band of rutile above anatase and the rutile-to-anatase photo-induced electron transfer. This work presents evidence supporting model (b).

[a] *Key Laboratory of Advanced Energy Materials Chemistry of the Ministry of Education, School of Material Science and Engineering, China*
[b] *Collaborative Innovation Center of Chemical Science and Engineering, Nankai University, Tianjin, 30071, P. R. China. E-mail: lild@nankai.edu.cn; Tel: +86-22-2350-0341*
[c] *Institute of Chemical Technology, University of Stuttgart, 70550 Stuttgart, Germany. E-mail: michael.hunger@itc.uni-stuttgart.de; Fax: +49-711-685-64081*

† Electronic supplementary information (ESI) available: Experimental details and characterization results. See DOI: 10.1039/c5cc04971g

alignment alternatively, *i.e.* both the conduction and valence bands in anatase are lower than those in rutile (Fig. 1b).[9] Thus, the photogenerated electrons would preferentially transfer from rutile to anatase, while the holes from anatase to rutile. The band alignment in anatase and rutile varies from ~0.2 eV[9a] and ~0.4 eV[9b,c] to even ~0.7 eV.[9d] In a recent study, bilayer anatase/rutile films with an effective interface contact were successfully synthesized and the reduction of silver by the trapped electrons on the anatase surface revealed the photo-induced electron transfer from rutile to anatase across the interface.[10]

Despite numerous theoretical calculations, the experimental evidence for the direction of charge transfer under irradiation in the mixed-phase TiO_2 is still lacking. Commercial mixed-phase TiO_2 Degussa P25 (TiO_2-P25) with *ca.* 80% anatase and 20% rutile (XRD patterns shown in Fig. S1, ESI†) is widely used as a benchmark semiconductor material in photocatalysis and it shows extremely high activity in most reactions. In fact, TiO_2-P25 is an ideal mixed-phase model to study the charge separation and transfer. Herein, we utilize ^{13}C-enriched ethanol as a probe molecule to investigate the specific surface sites of TiO_2-P25 using ^{13}C solid-state MAS (magic angle spinning) NMR spectroscopy, so as to give hints on the transfer of photo-induced electrons.

The TiO_2-P25 sample was firstly dehydrated in a vacuum at 673 K to remove the surface physisorbed and hydrogen-bonded water and other organic adsorbates. The sample was subsequently loaded with a certain amount of $CH_3{}^{13}CH_2OH$ and ^{13}C cross polarization MAS NMR measurement (CP/MAS) was performed to study the interaction of these molecules with the TiO_2 surface. Using this approach, the chemisorbed molecules can be easily distinguished from either physisorbed or gas-phase molecules since a CP/MAS spectrum will be significantly influenced by molecular mobility.[10] There are three significant signals appearing in the ^{13}C NMR spectra recorded after ethanol loading on mixed-phase TiO_2: a sharp signal at 58 ppm with a vague shoulder at 63 ppm due to the nonsymmetric outline of the narrow peak and a broad peak at 70 ppm (Fig. S2, ESI†). The narrow signal at 58 ppm is assigned to the methylene ($-CH_2-$) carbons of the major portion of ethanol molecules, which are either very mobile on the surface or exchange rapidly between the gas phase and the surface. The other ethanol molecules are immobilized on at least two different types of TiO_2 surface sites. Surface TiOH groups lead to the formation of strongly hydrogen-bonded ethanol, while coordinatively unsaturated Ti atoms lead to the formation of surface-bound Ti-ethoxide (CH_3CH_2O-Ti) species, originating the signals at 63 and 70 ppm.[11] With a short cross polarization contact time, the strongly bound molecules are preferentially detected. As a result, the relative intensity of the three signals changes with decreasing contact time. The signal at 58 ppm decreases dramatically, while the other two signals remain unaffected because the surface-bound ethoxides and hydrogen-bonded ethanol molecules are not involved in the fast exchange with molecules in the second monolayer. When the contact time decreases to 50 μs, the signal of the ethoxy species splits into two signals: a dominating signal at *ca.* 71 ppm and a weak signal at *ca.* 67 ppm, as shown in Fig. 2a. Considering that TiO_2-P25 is a mixed-phase TiO_2, the signals at 67 and

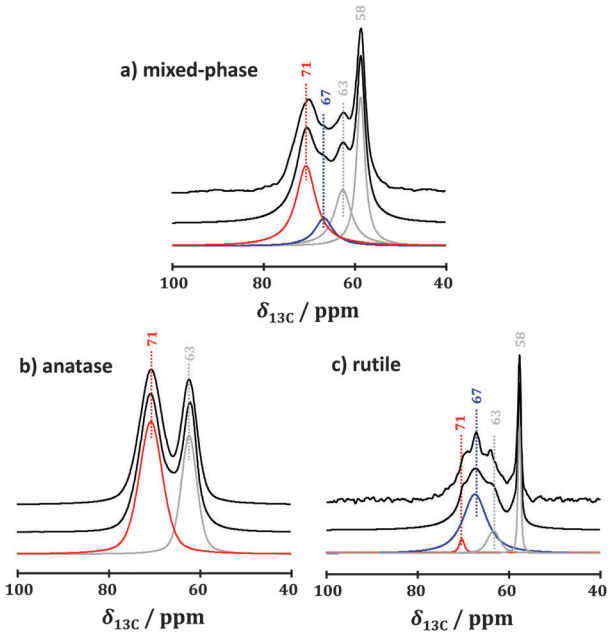

Fig. 2 ^{13}C CP/MAS NMR spectra of ethanol on dehydrated mixed-phase (a) TiO_2-P25, (b) rutile and (c) anatase. From top to bottom: experimental spectrum, simulated spectrum and deconvoluted components.

71 ppm might be due to the different surface configurations of anatase and rutile phases (Fig. S3, ESI†). It is interesting to note that the intensity ratio of the ^{13}C CP/MAS NMR signals of the ethoxy species on the surface of mixed-phase TiO_2 is calculated to be 79 : 21, in well accordance with the anatase/rutile ratio determined by XRD. In order to confirm this supposition, the ^{13}C CP/MAS NMR measurements of the ethanol loading on the surface of dehydrated rutile and anatase (XRD patterns shown in Fig. S1, ESI†) were performed. As shown in Fig. 2b, ethanol adsorption on the anatase surface gives two ^{13}C CP/MAS signals at 63 and 71 ppm, attributed to the hydrogen-bonded ethanol molecules and ethoxides bound to the coordinatively unsaturated Ti atoms on the anatase surface, respectively. For ethanol adsorption on the rutile surface (Fig. 2c), on the other hand, four ^{13}C CP/MAS signals at 58, 63, 67 and 71 ppm could be observed. The signals at 58 and 63 ppm are due to the mobile or gas phase and the hydrogen-bonded ethanol molecules, respectively. The dominating signal at 67 ppm is due to ethoxides bound to the coordinatively unsaturated Ti atoms on the rutile surface, while the weak shoulder signal at 71 ppm is due to the ethoxides bound to the residual anatase surface sites. It is known that the anatase phase can transform into the rutile phase at elevated temperatures, and phase transformation in the inner part of TiO_2 particles is relatively easier than in the outer part.[12] Since the rutile surface employed in this study was obtained from TiO_2-P25 through calcination at 1023 K for 12 hours (see the ESI† for details), traces of anatase may remain on the surface even though no XRD pattern corresponding to the anatase phase could be observed (Fig. S1, ESI†).

Based on the above-mentioned results, it is possible to distinguish the surfaces of anatase and rutile by MAS NMR spectroscopy using ethanol as a probe molecule. Afterwards,

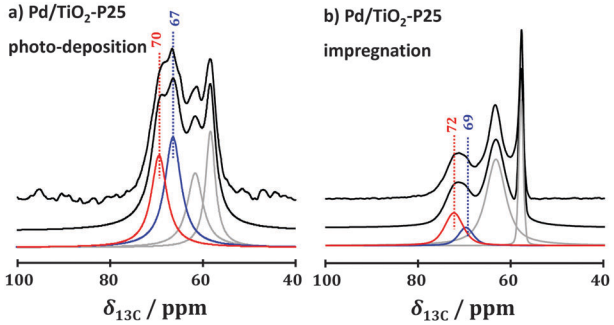

Fig. 3 ^{13}C CP/MAS NMR spectra of ethanol adsorption on dehydrated 2%Pd/TiO_2-P25 samples prepared *via* (a) photo-deposition and (b) wet-impregnation. From top to bottom: experimental spectrum, simulated spectrum and deconvoluted components.

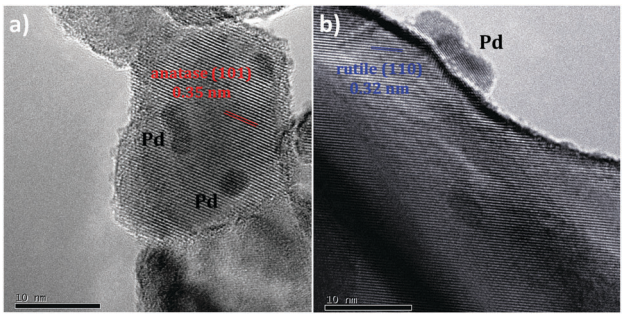

Fig. 4 HRTEM images of the 2%Pd/TiO_2-P25 samples prepared *via* (a) photo-deposition and (b) wet-impregnation.

the metal was introduced into mixed-phase TiO_2 *via* photo-deposition or wet-impregnation to partially cover the surface sites. For wet impregnation, metal clusters are expected to randomly cover the rutile and anatase surface sites *via* chemical or physical adsorption. In contrast, for photo-deposition, metal ions are selectively adsorbed on the surface through electrostatic interaction and are subsequently reduced by the photo-induced electrons to metal atoms (see Fig. S3 and ESI† for details).[13] In the case of mixed-phase TiO_2, the electrons and holes are created under irradiation, and separated in the anatase/rutile phase junction. Therefore, the metal atoms should go selectively to that TiO_2 phase, either anatase or rutile, where photo-induced electrons are accumulated (Fig. 1). The ^{13}C CP/MAS NMR spectrum recorded after the ethanol loading on 2%Pd/TiO_2-P25 samples prepared *via* photo-deposition is shown in Fig. 3a. A sharp decline in the exposed anatase surface sites could be observed, as indicated by the decrease in the relative intensity of the signal at *ca.* 71 ppm. The exposed anatase/rutile surface site ratio determined upon ethanol adsorption is found to be 45 : 55 for Pd/TiO_2-P25 prepared *via* photo-deposition, much lower than that for pristine TiO_2-P25 (79 : 21). The selective deposition of palladium on the anatase surface in mixed-phase TiO_2 *via* photo-deposition is further confirmed by microscopic observations. The high-resolution TEM (HRTEM) image of Pd/TiO_2-P25 prepared *via* photo-deposition (Fig. 4a) clearly shows that palladium clusters are located on the anatase {101} facets with an interplanar spacing of 0.35 nm. Since TEM is a microanalysis technique, we carefully examined as many HRTEM images and found that all observable palladium clusters were on the anatase surface in mixed-phase TiO_2-P25 (some representative HRTEM images are shown in Fig. S5, ESI†). In contrast, the exposed anatase/rutile surface site ratio is calculated to be 76 : 24 for Pd/TiO_2-P25 prepared *via* wet-impregnation using the ^{13}C CP/MAS NMR spectrum recorded after ethanol adsorption (Fig. 4b), very similar to 79 : 21 for pristine TiO_2-P25. It indicates a random deposition of palladium metal clusters on both anatase and rutile surfaces during the wet-impregnation, as previously expected. Meanwhile, the palladium cluster located on rutile {110} with an interplanar spacing of 0.32 nm could be observed for Pd/TiO_2-P25 prepared *via* wet-impregnation, as shown in Fig. 4b. More TEM images show that wet-impregnated palladium clusters are randomly loaded on the anatase surface, rutile surface or the anatase/rutile interface (Fig. S5, ESI†).[14]

The results of NMR spectroscopy and TEM analysis clearly confirm the selective deposition of palladium metal clusters on the surface of anatase during the photo-deposition process. Further results of NMR spectroscopy reveal that the selective deposition of metal clusters on the anatase surface can be achieved for several other metals, *e.g.* Pt, Ir and Ag (Fig. S6, ESI†). These experimental observations evidence the rutile-to-anatase transfer of photo-induced electrons and undoubtedly support the energetic alignment shown in Fig. 1b.

In summary, with ethanol as a probe molecule, the surface sites of anatase and rutile in mixed-phase TiO_2 are successfully distinguished using ^{13}C CP/MAS NMR spectroscopy. The selective photo-deposition of metal clusters on the anatase surface in mixed-phase TiO_2 is disclosed by monitoring the changes in the exposed anatase/rutile surface sites before and after photo-deposition, which clearly indicates a rutile-to-anatase photo-induced electron transfer in mixed-phase TiO_2 and strongly evidences a staggered band alignment with both bands of rutile higher than those of anatase.

This work is supported by the National Natural Science Foundation of China (21421001), the Ministry of Education of China (IRT13022) and the 111 project (B12015). Furthermore, M.H. wants to thank for the financial support from Deutsche Forschungsgemeinschaft (HU533/13-1).

Notes and references

1 A. Fujishima and K. Honda, *Nature*, 1972, **238**, 37.
2 (*a*) J. Pascual, J. Camassel and H. Mathieu, *Phys. Rev. B: Condens. Matter Mater. Phys.*, 1978, **18**, 5606; (*b*) H. Tang, H. Berger, P. Schmid, F. Levy and G. Burri, *Solid State Commun.*, 1993, **87**, 847.
3 (*a*) U. Diebold, *Surf. Sci. Rep.*, 2003, **48**, 53; (*b*) A. Fujishima, X. Zhang and D. A. Tryk, *Surf. Sci. Rep.*, 2008, **63**, 515.
4 (*a*) J. Zhang, Q. Xu, Z. Feng, M. Li and C. Li, *Angew. Chem., Int. Ed.*, 2008, **47**, 1766; (*b*) T. Ohno, K. Sarukawa, K. Tokieda and M. Matsumura, *J. Catal.*, 2001, **203**, 82; (*c*) T. Ohno, K. Tokieda, S. Higashida and M. Matsumura, *Appl. Catal., A*, 2003, **244**, 383; (*d*) G. H. Li, S. Ciston, Z. V. Saponjic, L. Chen, N. M. Dimitrijevic, T. Rajh and K. A. Gray, *J. Catal.*, 2008, **253**, 105.
5 (*a*) X. Wang, Q. Xu, M. Li, S. Shen, X. Wang, Y. Wang, Z. Feng, J. Shi, H. Han and C. Li, *Angew. Chem., Int. Ed.*, 2012, **51**, 13089; (*b*) J. Zhang, M. Zhang, R. Sun and X. Wang, *Angew. Chem., Int. Ed.*, 2012, **51**, 10145.

6 L. Kavan, M. Grätzel, S. E. Gilbert, C. Klemenz and H. J. Scheel, *J. Am. Chem. Soc.*, 1996, **118**, 6716.
7 (*a*) T. Kawahara, Y. Konishi, H. Tada, N. Tohge, J. Nishii and S. Ito, *Angew. Chem., Int. Ed.*, 2002, **41**, 2811; (*b*) H. Nakajima, T. Mori, Q. Shen and T. Toyoda, *Chem. Phys. Lett.*, 2005, **409**, 81; (*c*) J. Kang, F. M. Wu, S. S. Li, J. B. Xia and J. B. Li, *J. Phys. Chem. C*, 2012, **116**, 20765; (*d*) S. Shen, X. L. Wang, T. Chen, Z. C. Feng and C. Li, *J. Phys. Chem. C*, 2014, **118**, 12661.
8 (*a*) D. C. Hurum, A. G. Agrios, K. A. Gray, T. Rajh and M. C. Thurnauer, *J. Phys. Chem. B*, 2003, **107**, 4545; (*b*) D. C. Hurum, K. A. Gray, T. Rajh and M. C. Thurnauer, *J. Phys. Chem. B*, 2005, **109**, 977.
9 (*a*) M. G. Ju, G. X. Sun, J. J. Wang, Q. Q. Meng and W. Z. Liang, *ACS Appl. Mater. Interfaces*, 2014, **6**, 12885; (*b*) P. Deák, B. Aradi and T. Frauenheim, *J. Phys. Chem. C*, 2011, **115**, 3443; (*c*) D. O. Scanlon, C. W. Dunnill, J. Buckeridge, S. A. Shevlin, A. J. Logsdail, S. M. Woodley, C. R. A. Catlow, M. J. Powell, R. G. Palgrave, I. P. Parkin, G. W. Watson, T. W. Keal, P. Sherwood, A. Walsh and A. A. Sokol, *Nat. Mater.*, 2013, **12**, 798; (*d*) V. Pfeifer, P. Erhart, S. Y. Li, K. Rachut, J. Morasch, J. Brotz, P. Reckers, T. Mayer, S. Rühle, A. Zaban, I. M. Sero, J. Bisquert, W. Jaegermann and A. Klein, *J. Phys. Chem. Lett.*, 2013, **4**, 4182.
10 R. Quesada-Cabrera, C. Sotelo-Vazquez, J. C. Bear, J. A. Darr and I. P. Parkin, *Adv. Mater. Interfaces*, 2014, **1**, 1400069.
11 (*a*) S.-J. Hwang and D. Raftery, *Catal. Today*, 1999, **49**, 353; (*b*) S. Pilkenton, S.-J. Hwang and D. Raftery, *J. Phys. Chem. B*, 1999, **103**, 11152.
12 (*a*) J. Shi, J. Chen, Z. Feng, T. Chen, Y. Lian, X. Wang and C. Li, *J. Phys. Chem. C*, 2007, **111**, 693; (*b*) J. Zhang, Q. Xu, M. Li, Z. Feng and C. Li, *J. Phys. Chem. C*, 2009, **113**, 1698.
13 (*a*) F. Zhang, N. Guan, Y. Li, X. Zhang, J. Chen and H. Zeng, *Langmuir*, 2003, **19**, 8230; (*b*) F. Zhang, J. Chen, X. Zhang, W. Gao, R. Jin and N. Guan, *Catal. Today*, 2004, **93–95**, 645; (*c*) R. Li, F. Zhang, D. Wang, J. Yang, M. Li, J. Zhu, X. Zhou, H. Han and C. Li, *Nat. Commun.*, 2013, **4**, 1432.
14 (*a*) D. Tsukamoto, Y. Shiraishi, Y. Sugano, S. Ichikawa, S. Tanaka and T. Hirai, *J. Am. Chem. Soc.*, 2012, **134**, 6309; (*b*) Y. Shiraishi, K. Fujiwara, Y. Sugano, S. Ichikawa and T. Hirai, *ACS Catal.*, 2013, **3**, 312.

